

Electrical conductivity of thin film ceria grown by pulsed laser deposition

Jong Hoon Joo, Gyeong Man Choi*

Fuel Cell Research Center, Department of Materials Science and Engineering, Pohang University of Science and Technology, Pohang, Gyeongbuk 790-784, Republic of Korea

Available online 19 March 2007

Abstract

Gd-doped ceria (GDC) thin films, 0.5–1.8 μm thick, were deposited on Pt and sapphire substrates by pulsed laser deposition (PLD) method. The in-plane and the perpendicular-to-plane conductivities (hereafter, “across-plane” conductivity) of thin films were measured and compared to that of bulk sample. X-ray diffraction and electron microscopy results showed that the films on Pt and sapphire were polycrystalline cubic with a columnar structure. The grain conductivities of the GDC films, obtained from the impedance spectra of in-plane and across-plane measurements, were slightly lower than that of the GDC bulk. However, very little difference in conductivity was shown between films, regardless of substrates and measurement modes. The activation energies and the P_{O_2} dependence of the GDC thin films were similar to that of bulk GDC. In the low temperature range, the GDC films exhibited conductivities about one order of magnitude higher than that of the YSZ (Yttria-stabilized zirconia) film.

© 2007 Elsevier Ltd. All rights reserved.

Keywords: CeO₂; Film; Electrical conductivity; Fuel Cells; PLD

1. Introduction

Solid oxide fuel cells (SOFCs) have been rapidly developing for clean and efficient power generation using a variety of fuels. With the advent of thin film technology, efforts have been made to make miniaturized SOFCs.^{1,2} Miniaturized SOFCs are potentially high efficiency, having high energy-density replacements for batteries in the mW–W power generation for portable consumer and military electronic devices. Miniaturized SOFCs offer great advantages over their macroscopic counterparts such as low operating temperature, easy integration with the required electrical components, small size and reduced weight.³ Recently, considerable efforts have also been directed to intermediate-temperature SOFCs based on thin-film electrolytes of doped ceria. Rare-earth oxide-doped ceria is one of the candidates for the electrolytes of intermediate temperature SOFCs.⁴

The electrical characterization of thin film conductivity is more complicated than that of bulk since thin film cannot be prepared without substrate. Two different geometrical approaches can be used for the electrical measurements. The first approach

is based on measurement of conductivity perpendicular to the film plane (“across-plane conductivity”). In this geometry the contact problem may influence the conductivity.⁵ Impedance spectroscopy is the only way to differentiate the effect of contact resistance on the overall resistance. The second approach is based on in-plane measurements (“in-plane conductivity”). In this case substrates with high resistance should be used. For this geometry, two-probe direct-current measurements can be employed because the contact resistance is relatively small, compared to the film resistance and grain, and grain boundary resistances can not be separated due to the capacitance of the substrate.^{6,7}

Compared with doped-zirconia such as YSZ, fewer studies have been done on doped-ceria such as GDC films, in part because of the difficulty in obtaining uniform, continuous and high quality film.^{8–11} Very few works deal with the across-plane conductivity of the GDC film. The across-plane conductivity characterization is important since current flows perpendicular to film plane during the SOFC operation. In addition, there are contradictions in the conductivity of GDC thin films among the authors. Chen et al.⁸ who investigated GDC20 ($\text{Ce}_{0.8}\text{Gd}_{0.2}\text{O}_{2-\delta}$) thin films prepared by PLD on MgO substrate, reported that the film conductivity did not significantly depend on P_{O_2} in the range from 1 to 10^{-19} atm at 655–818 °C. On the contrary, Suzuki et al.¹⁰ who investigated GDC20 thin films prepared by a sol–gel

* Corresponding author. Tel.: +82 54 279 2146; fax: +82 54 279 2399.
E-mail address: gmchoi@postech.ac.kr (G.M. Choi).

process on sapphire substrate, reported that the film conductivity followed $P_{O_2}^{-1/4}$ behavior at P_{O_2} in the range from 10^{-13} to 10^{-20} atm at 800°C .

In this study, GDC thin films were deposited on Pt and sapphire substrates by pulsed laser deposition method. Across-plane and in-plane conductivities of thin films were measured and compared to that of bulk sample.

2. Experimental procedures

GDC films were deposited on Pt and sapphire substrates using PLD method at oxygen partial pressure of ~ 50 mTorr. The films were deposited on the commercially available Pt (1 1 1)/TiO₂/SiO₂/Si and sapphire (0 0 1) substrates. A stainless steel chamber was evacuated to a base pressure of 5×10^{-6} Torr. Pulsed laser ablation was carried out with a KrF excimer laser (248 nm with 30 ns pulse width) at the energy of ~ 1.5 J/cm² and the repetition rate of 10 Hz. To avoid cracking films during the film deposition, the GDC film on Pt (1 1 1) substrate was grown at 500°C , and the film on sapphire (0 0 1) was grown at 700°C . For electrical measurements of across-plane conductivity, 0.03 cm² Pt electrode was sputtered on the surface of thin film.

The electrical conductivities of the films were measured as a function of temperature and P_{O_2} using impedance and two-probe d.c. method. The impedance spectra were obtained by using an impedance analyzer (Model 4192a, Japan) and an impedance Gain-Phase Analyzer (Solartron SI 1260, UK). The P_{O_2} dependence of conductivity was measured for the P_{O_2} range of 1×10^{-27} atm between 600 and 700°C . The phase of thin film was characterized by X-ray diffraction (XRD) using Cu K α radiation (MAC Science, M18XCE, Japan). Microstructure observation was performed by a field-emission scanning electron microscope (JEOL, Model 3330F, Japan). Average column diameter was estimated by using the linear intercept method by counting more than 200 grains. The compositions were also confirmed by using a FE-SEM equipped with an energy dispersive X-ray spectroscopy system (EDS).

3. Results and discussion

Fig. 1 shows XRD patterns of GDC bulk and thin films deposited on Pt (1 1 1) and sapphire (0 0 1) substrates. The XRD patterns obtained from the films were consistent with the reference data for single phase GDC with cubic fluorite structure of bulk GDC20. Peaks due to different substrates were also observed. The polycrystalline-cubic nature of the films is apparent in XRD patterns. No secondary phases due to film/substrate interaction were detected. It was also found that the crystal orientation changed with substrate. A strongly preferential orientation of (1 1 1) planes in the film was obtained on sapphire (0 0 1) substrate.

Fig. 2 shows the surface (left) and cross-sectional (right) SEM micrographs of GDC thin films deposited on (a) Pt (1 1 1) and (b) sapphire (0 0 1) substrates. Although the columnar growth of the grain is shown for all films, the columnar nature is

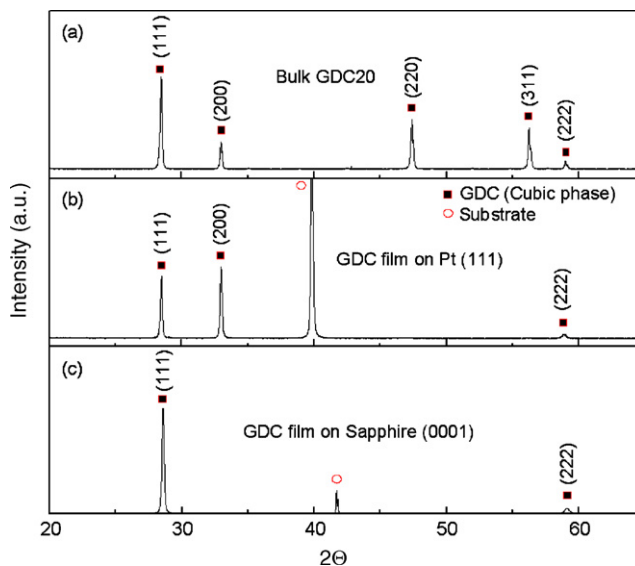


Fig. 1. XRD patterns of (a) GDC bulk for comparison and thin films deposited on (b) Pt (1 1 1) and sapphire (0 0 1) substrates.

less apparent for the film grown on a sapphire substrate. Since these films have columnar structures, the grain size measured from the surface view represents the diameter of the columns. Nanocrystalline morphology was observed with an average column diameter of ~ 90 nm as shown in Fig. 2(a). Well-crystallized GDC thin film was also obtained on sapphire (0 0 1) substrates with an average grain size of ~ 40 nm as shown in Fig. 2(b). Thin film GDC had Gd atomic contents of $\sim 21\%$, i.e., Ce_{0.79}Gd_{0.21}O_{2- δ} , determined by EDS. Thus, for the fully oxidized GDC thin films, the film composition was \sim GDC21, close to GDC20 target.

The electrical conductivities of the thin films and bulk GDC were investigated by impedance spectroscopy. For electrical measurements of across-plane conductivity, Pt electrode was sputtered on the surface of the GDC film. Pt electrode was ~ 150 nm thick with areas of 0.03 cm². The incomplete contact at the Pt/GDC film interface can cause the conductivity drop in thin film. Since Pt electrode shows negligible pinholes in the shown scale, the low measured conductivity due to the porous electrode is not likely. Fig. 3 compares the impedance spectra obtained for thin film and bulk GDC in dry air at 200°C . The impedance spectrum of thin film consists of a high-frequency semicircle caused by a grain process and a low-frequency curve attributed to the interface between GDC film and sputtered Pt electrode. The spectra were analyzed by using an equivalent circuit shown in Fig. 3. A series connection of R_1Q_1 and R_2Q_2 was used where R_i is the resistance and Q_i is the constant-phase element. A fitting line was drawn for the film grown on Pt (1 1 1) substrate. To confirm the grain conductivity in the thin film, the relative dielectric permittivity (ϵ_r) was obtained from the peak of the high frequency semicircle. The ϵ_r value of GDC film on Pt (1 1 1) was ~ 50 . Although a small grain boundary contribution was shown at intermediate frequencies for bulk GDC, no grain boundary contribution was observed for the film. This difference may partly be due to the columnar structure of thin film, in which the grain boundary is parallel to the current direction.¹²

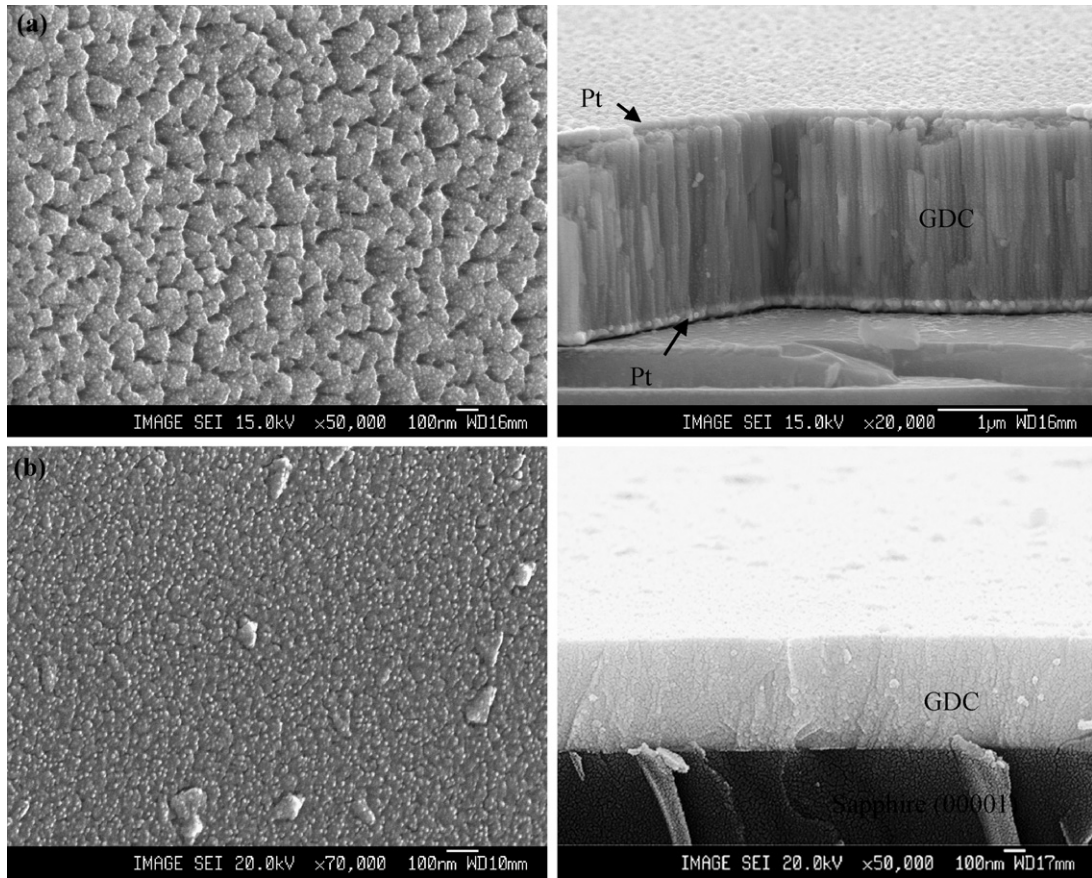


Fig. 2. Surface (left) and cross-sectional (right) SEM micrographs of the GDC thin films grown on (a) Pt (111) and (b) sapphire (0001) substrates. Scale bars are 100 nm, except for 1 μm bar in upper-right figure.

In order to calculate the conductivity of film, the resistance of Pt electrode was separately measured and subtracted.

For the electrical measurements of in-plane conductivity, substrates with high resistance need to be used. The measured conductance of the sapphire substrate was about three orders lower than that of the GDC film at 700 °C. Fig. 4 compares the impedance spectra obtained for the thin film on sapphire and bulk GDC by taking the geometrical factor into consideration at 700 °C. Only one semicircle was observed in the spectra measured under in-plane mode. The electrode resistance was not observed since it is negligible compared to the

GDC film resistance due to the small geometrical factor, A/ℓ (area/length) $\sim 1.7 \times 10^{-4}$, and thus the large resistance of thin film. On the other hand, due to large geometrical factor (~ 1) and thus small resistance of bulk GDC sample, electrode resistance was not negligible and thus shown in an impedance plane. The calculated capacitance ($\sim 10^{-11}$ F) of GDC thin film was similar to the substrate capacitance. Thus the impedance spectrum cannot distinguish between the effect of film sample and substrate. Only the total resistance value can be obtained by impedance spectrum analysis. Fig. 4 shows a good agreement between the resistivity values obtained by a.c. and d.c. measurements for the GDC thin film. The grain boundary effect

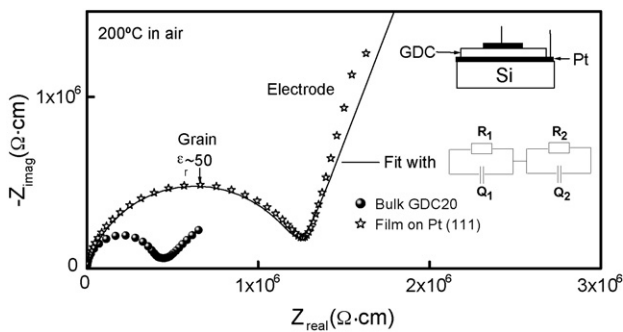


Fig. 3. Impedance spectra in across-plane mode of thin films deposited on Pt (111) substrate were compared to that of the bulk GDC at 200 °C in air. The equivalent circuit used for fitting the data was also shown.

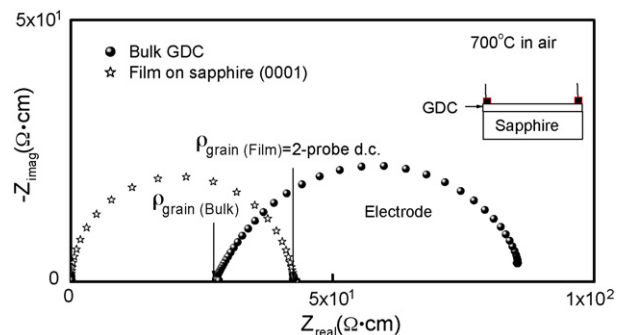


Fig. 4. Impedance spectra of GDC thin film on sapphire, measured under in-plane mode, was compared to that of bulk GDC at 700 °C in dry air.

may not be neglected since current flow is now perpendicular to the columnar grains. However, impedance spectrum analysis in the in-plane conductivity cannot separate the grain from the grain boundary contribution due to the insulating substrate. We may only estimate the effect of the grain boundary by considering other properties. The activation energy of the film (0.86 ± 0.001 eV, ≥ 500 °C) on sapphire was similar to or slightly higher than that of the bulk grain (0.76 ± 0.004 eV, ≥ 500 °C). In addition, negligible grain boundary contribution was shown for the bulk GDC that was used as a target. Thus we conclude that the total conductivity of the film on sapphire was mostly determined by the grain conductivity.

The measurement of the film conductivity as a function of P_{O_2} and temperature may confirm the quality of the GDC film. Fig. 5 shows that the plot of $\log \sigma$ versus $\log P_{O_2}$ can be divided into two regions. In the high- P_{O_2} region, the conductivity is independent of P_{O_2} . In this region, the electrical conductivity is predominantly ionic. In the low- P_{O_2} region, the conductivity increases with decreasing P_{O_2} due to the electronic conduction. The conductivity can be expressed by the sum of P_{O_2} -independent ionic (σ_{ion}) and $P_{O_2}^{-1/4}$ -dependent electronic (σ_e) conductivity. The P_{Θ} of the GDC film, which represents the oxygen partial pressure at which $\sigma_{ion} = \sigma_e$, has a value $\sim 10^{-23.2}$ atm at 600 °C, similar to the reported value $\sim 10^{-22.4}$ atm for the GDC20 bulk.⁴ Thus film shows a similar conductivity curve to a bulk sample.

Fig. 6 compares the grain conductivity of thin films. For comparison, the grain conductivity of the bulk GDC20 and other reported data of the GDC20 thin films and 8YSZ (8 mol% Y_2O_3 -doped ZrO_2) thin film were also shown.^{6,8,10,11} All the reported data of the GDC20 film, representing total (grain and grain boundary) conductivities, were obtained from in-plane measurement. Across-plane measurement is difficult due to the leakage through thin film unless the film has a good quality. In this study, the grain conductivities of the GDC films, obtained from the impedance spectra of in-plane and across-plane measurement, were slightly lower than that of GDC bulk. However, very little difference in conductivity was shown between films, regardless of substrates and measurement mode. The activation

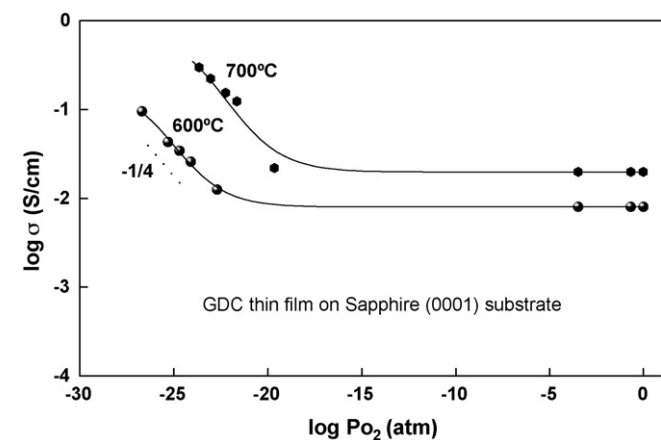


Fig. 5. The electrical conductivity of GDC thin film on sapphire was plotted as a function of oxygen partial pressure (P_{O_2}) and temperature (600 and 700 °C).

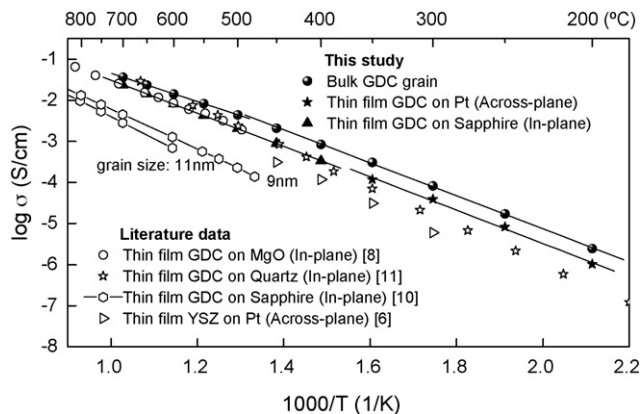


Fig. 6. The grain conductivities of GDC thin films, both in-plane and across-plane modes, and that of bulk GDC20 measured in this study, as a function of temperature, were compared (filled symbols). Literature data for thin films (GDC20 and 8YSZ) were also shown for comparison (open symbols).

energies of the GDC thin films deposited on Pt (1 1 1), sapphire (0 0 1) were 0.85 ± 0.03 ($200 < T < 450$ °C), 0.86 ± 0.001 eV ($T > 500$ °C), and those of the bulk GDC were 0.76 ± 0.004 ($T > 500$ °C), 0.84 ± 0.007 eV ($T < 500$ °C), respectively, as indicated by the solid fitting line. Thus, both the across-plane conductivity curve, obtained at a low temperature and the in-plane conductivity curve, obtained at a high temperature, become nearly straight lines when connected. Both the activation energy and the P_{O_2} -dependence of the GDC thin film were similar to that of the bulk GDC. In the low temperature range (300–450 °C), the GDC films exhibit conductivities about one order of magnitude higher than that of the YSZ film.

4. Conclusions

Well-crystallized GDC thin films were successfully fabricated on Pt and sapphire substrates by using PLD method. The across-plane conductivity measurement became possible and the conductivity was similar to the conductivities of film in in-plane mode. X-ray diffraction and electron microscopy results showed that the films on Pt and sapphire were polycrystalline cubic with columnar structure. The grain conductivities of the GDC films, obtained from the impedance spectra of in-plane and across-plane measurements, were slightly lower than that of GDC bulk. However, very little difference in conductivity was shown between films, regardless of substrates and measurement modes. The activation energy and the P_{O_2} dependence of the GDC thin films were similar to that of bulk GDC. Thus we may conclude that there is no unusual observation such as the conductivity enhancement or the appearance of electronic conductivity in high P_{O_2} for nano-crystalline GDC films in this study. Our conclusion may be limited to the grain size or column diameter of 40–90 nm. In the low temperature range (300–450 °C), the GDC films exhibit conductivities about one order of magnitude higher than that of the YSZ film. From the observation in this study, we believe the GDC film can be a good electrolyte material for low-temperature SOFCs.

Acknowledgements

This work was supported by Core Technology of Fuel Cell Program, MOCIE and POSRIP Program of POSTECH, Korea.

References

1. Hertz, J. L. and Tuller, H. L., Electrochemical characterization of thin films for a micro-solid oxide fuel cell. *J. Electroceram.*, 2004, **13**, 663–668.
2. Lao, G. J., Hertz, J. L., Tuller, H. L. and Horn, Y. S., Microstructural features of RF-sputtered SOFC anode and electrolyte materials. *J. Electroceram.*, 2004, **13**, 691–695.
3. Baertsch, C. D., Jensen, K. F., Hertz, J. L., Tuller, H. L., Vengallatore, S. T., Spearing, S. M. *et al.*, Fabrication and structural characterization of self-supporting electrolyte membranes for a micro solid-oxide fuel cell. *J. Mater. Res.*, 2004, **19**, 2604–2615.
4. Steele, B. C. H., Appraisal of $\text{Ce}_{1-y}\text{Gd}_y\text{O}_{2-y/2}$ electrolytes for IT-SOFC operation at 500 °C. *Solid State Ionics*, 2000, **129**, 95–110.
5. Kwon, O. H. and Choi, G. M., Electrical conductivity of thick film YSZ. *Solid State Ionics*, 2006, **177**, 3057–3062.
6. Joo, J. H. and Choi, G. M., Electrical conductivity of YSZ thin film grown by pulsed laser deposition. *Solid State Ionics*, 2006, **177**, 1053–1057.
7. Petrovsky, T., Anderson, H. U. and Petrovsky, V., Impedance spectroscopy and direct current measurements of YSZ films. *Mater. Res. Soc. Symp. Proc.*, 2003, **756**, EE4.7.1–EE4.7.6.
8. Chen, L., Chen, C. L., Chen, X., Donner, W., Liu, S. W., Lin, Y. *et al.*, Electrical properties of a highly oriented, textured thin film of the ionic conductor $\text{Gd}:\text{CeO}_{2-\delta}$ on (001) MgO. *Appl. Phys. Lett.*, 2003, **83**, 4737–4739.
9. Chen, L., Chen, C. L., Huang, D. X., Lin, Y., Chen, X. and Jacobson, A. J., High temperature electrical conductivity of epitaxial Gd-doped CeO_2 thin films. *Solid State Ionics*, 2004, **175**, 103–106.
10. Suzuki, T., Kosacki, I. and Anderson, H. U., Microstructure-electrical conductivity relationships in nanocrystalline ceria thin films. *Solid State Ionics*, 2002, **151**, 111–121.
11. Chiodelli, G., Malavasi, L., Massarotti, V., Mustarelli, P. and Quartarone, E., Synthesis and characterization of $\text{Ce}_{0.8}\text{Gd}_{0.2}\text{O}_{2-y}$ polycrystalline and thin film materials. *Solid State Ionics*, 2005, **176**, 1505–1512.
12. Kek, D., Panjan, P., Wanzenberg, E. and Jamnik, J., Electrical and microstructural investigations of cermet anode/YSZ thin film systems. *J. Eur. Ceram. Soc.*, 2001, **21**, 1861–1865.